

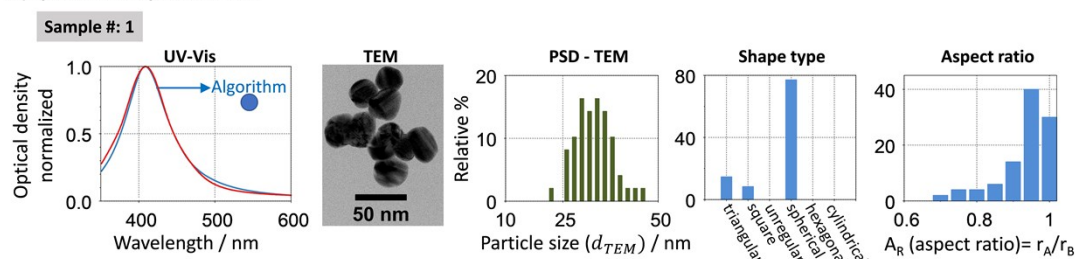
Continuous manufacturing of silver nanoparticles between 5 and 80 nm with rapid online optical size and shape evaluation

Bruno Pinho, Laura Torrente-Murciano¹

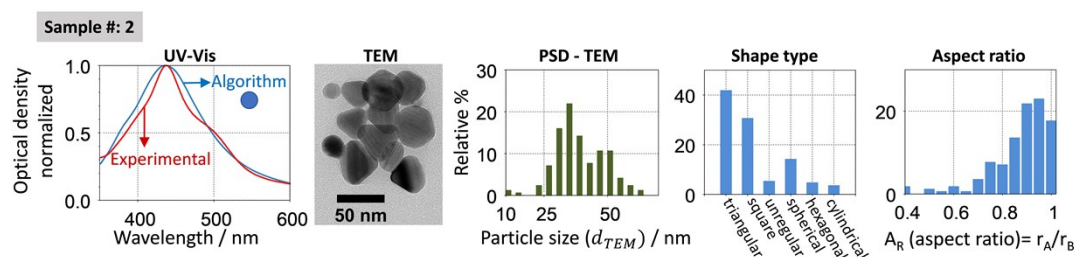
Department of Chemical Engineering and Biotechnology, University of Cambridge, Philippa Fawcett Drive, CB3 0AS, Cambridge, UK

Supplementary information

A) Spherical and spheroidal NPs



B) Non-spherical NPs



C) Series of non-spherical and spherical particles

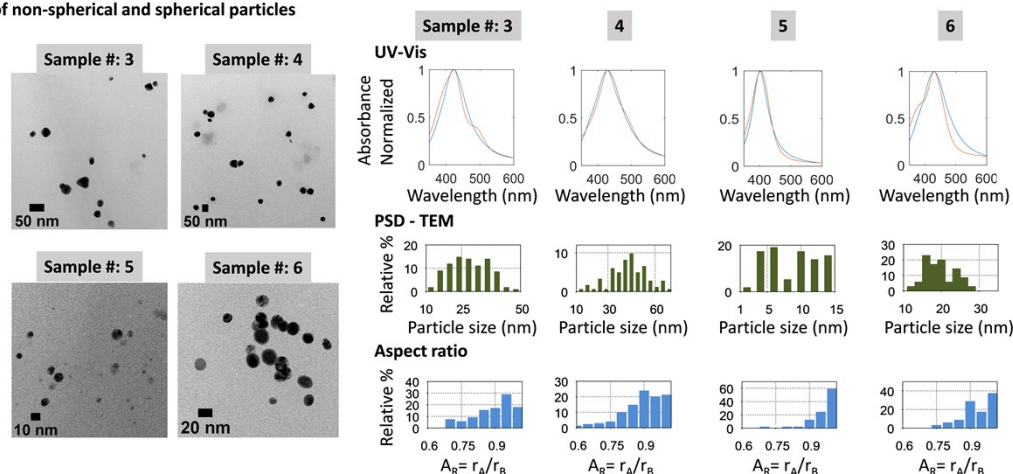


Figure S1: Experimental data of synthesized particles with different shapes (A – non-spherical and B – spherical and spheroidal) used to define the best quality parameter. C) Set of synthesized samples with spherical and non-spherical characteristics.

¹ Corresponding author: lt416@cam.ac.uk

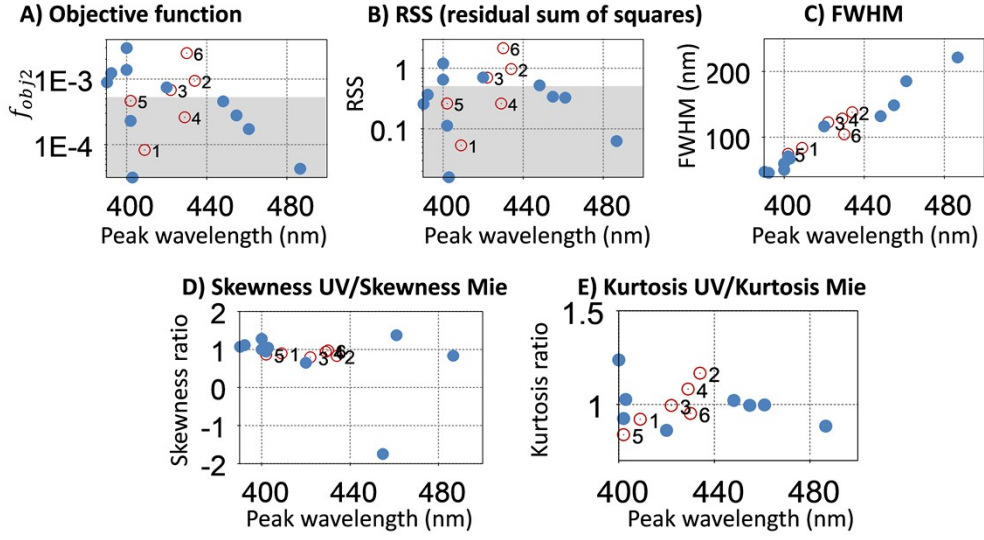


Figure S2: Comparison of different parameters for "spherical degree" using ~ spherical (spheres and spheroids) and non-spherical synthesized citrate-based silver particles (o) and spherical citrate-based commercial particles (●). The grey zone was here defined by visual inspection, as the first attempt to define a zone with spherical particles. The characterization of the "o" set is present in Figure S1).

Derivate objective function

The simplest form of the objective function is constructed by minimizing the difference between the experimental results (UV-Vis measurements) and their simulated ones (from Mie theory). The least-square method was applied to a monodisperse spherical nanoparticle sample:

$$f_{obj} = \min_r \sum_{\lambda_0}^{\lambda_f} \left(\frac{\ln(I_0/I)_\lambda}{Exp. data} - \frac{\sigma_{ext}(\lambda, r, \epsilon) L C_p}{Lambert Beer law} \right)^2 \quad \text{Eq. S1}$$

where $(I_0/I)_\lambda$ is the experimental extinction response of monochromatic light at wavelength λ , L [m] is the optical length, C_p is the total number of particles per volume of solution [particles·m_{sol}⁻³] and σ_{ext} [m²] is the extinction cross-section of a single particle, which can be evaluated using Mie theory. If multiple scattering interactions can be neglected, the Eq. S1 can be adapted to a particle size distribution (PSD), being now defined as:

$$f_{obj} = \min_{f(r) \wedge r} \sum_{\lambda_0}^{\lambda_f} \left(\frac{\ln(I_0/I)_\lambda}{Exp. data} - \frac{LN_p \frac{3}{4} \int_{r_0}^{r_f} \frac{Q_{ext}(\lambda, r, \epsilon) PSD}{r f(r)} d(r)}{Lambert Beer law} \right)^2 \quad \text{Eq. S2}$$

$$\sum_{r_0}^{r_f} f(r) = 1, \quad 0 \leq f(r) \leq 1 \quad \text{Eq. S3}$$

where r is a single radius evaluated of the PSD, and $f(r)$ is the volume frequency distribution. Eq. S2 has to account for dielectric variations by chemical interaction with the medium, which can lead to a shift in the spectra position (λ_{shift} [nm]). The objective function is now defined as:

$$f_{obj} = \min_{f(r) \wedge r} \left(\sum_{\lambda_0}^{\lambda_f} \left(\ln(I_0/I)_{\lambda + \lambda_{shift}} - \frac{RSS}{\sum_{\lambda_0}^{\lambda_f} \left(\ln(I_0/I)_{\lambda + \lambda_{shift}} - \frac{LN \int_{r_0}^{r_f} \frac{Q_{ext}(\lambda, r, \epsilon)^{PSD}}{r} d(r)}{f(r)} \right)^2} \right) \right)^2 \quad \text{Eq. S4}$$

$$\lambda_{shift} = \lambda^{\max(I/I_0)} - \lambda^{\max(\text{Calculated})} \quad \text{Eq. S5}$$

where RSS is the residual sum of squares. Eq. S4 is a classical inverse problem (or ill-posed) defined as the Fredholm integral equation of first kind, which is highly sensitivity towards small errors and experimental noise in the input data, often leading to under- or over- solutions. Tikhonov regularization method is one of the most used strategies to reduce the effects of ill-conditioning problems by adding a smoothing function (or regularization term), which captures a compromise between solution accuracy and stability.

$$f_{obj.} = \min_{f(r) \wedge r} \left(RSS + \alpha \|f(r)\|_2^2 \right) \quad \text{Eq. S6}$$

where α is the Tikhonov regularization parameter which controls the weight between RSS and the regularization term. Previously, in Eq. S4 and S5, the shift was introduced as a way to account for changes in the peak location due to changes in the chemical environment. No boundaries were introduced to this shift, which allows spectra to shift without restriction in order to provide the best fitting results for peak shape. This is not completely accurate, and a restriction should be added to balance the weight (β) between peak location ($|\lambda_{shift}|$) and peak fit (Eq. S6). In this sense, the following equation was defined as an attempt to make the expression relative.

$$f_{obj.} = \min_{f(r) \wedge r} \left(\beta \frac{RSS + \alpha \|f(r)\|_2^2}{\sum_{\lambda_0}^{\lambda_f} \ln(I_0/I)_{\lambda + \lambda_{shift}}} + (1 - \beta) |\lambda_{shift}| \right) / \lambda^{\max(I/I_0)} \quad \text{Eq. S7}$$

where β ($0 \leq \beta \leq 1$) is an empirical weight defined by the user.

With optimized $A(r)$
 $A(r) = -3.30 \times 10^{-1} + 4.10 \times 10^{-1}r - 3.20 \times 10^{-3}r^2 - 5.69 \times 10^{-4}r^3$

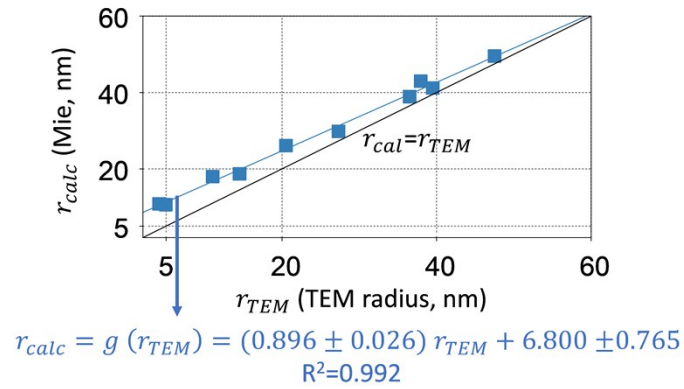


Figure S3: Calibration curve $[g(r_{TEM})]$ of Mie theory average particle size using commercial and synthesized particle standards. The curve is generated using an optimized damping coefficient, $A(r)$, which modifies the dielectric function response. By applying $A(r)$ and $g(r_{TEM})$ to the particle size algorithm, Mie theory size-extinction matrix (σ_{ext}) is now close to the standards.